



ELSEVIER

Contents lists available at [ScienceDirect](http://www.sciencedirect.com)

## Mechanics of Materials

journal homepage: [www.elsevier.com/locate/mechmat](http://www.elsevier.com/locate/mechmat)

CrossMark

HPSTAR  
094-2015

# Spallation caused by the diffusion and agglomeration of vacancies in ductile metals

Yuanjie Huang\*

The National Key Laboratory of Shock Wave and Detonation Physics, Institute of Fluid Physics, Chinese Academy of Engineering Physics, Mianyang 621900, China  
Center for High Pressure Science and Technology Advanced Research, Shanghai 201203, China

## ARTICLE INFO

## Article history:

Received 1 March 2014

Received in revised form 9 December 2014

Available online 18 December 2014

## Keywords:

Spallation

Ductile metals

Damage

Void

## ABSTRACT

In this paper, the spallation process for the ductile metals under plane shock loading is discussed in theory. By employing the phase transition theory and non-equilibrium theory, the spallation process may be understood as a result of the diffusion and agglomeration of the generated vacancies. Through the detailed theoretical analysis, the following important points are concluded: (1) the spalling temperature, a new concept, is proposed first and the appearance of spallation critical behavior is proved; (2) the quantitative grain size, tensile strain rate and temperature dependence of both the damage evolution rate and the void growth velocity is obtained; (3) the existence of a characteristic size for the voids and a characteristic stress at the void boundary is discovered first, and their magnitude depend on the vacancy excitation energy and the average volume of one vacancy; (4) the temperature of metal near the growing void is found to be high, possibly causing the metal to melt, and it decreases quickly with the distance away from the void; (5) the area of the plastic zone, surrounding one formed spherical void, is clarified; (6) the viewpoint is put forward that the void growth may arise from the agglomeration of vacancies rather than the emission of dislocations when the shocking temperature approaches spalling temperature. Most of the above theoretical results are novel and obtained first.

© 2014 Elsevier Ltd. All rights reserved.

## 1. Introduction

Due to the wide spectrum of issues ranging across defense and industrial applications, material behaviors at high pressure, high strain and high strain-rate physical processes, e.g. spallation process, is interesting in science. For the ductile metal in the spallation process, typically possessing the above extreme physical conditions, the dynamic damage occurs and is experimentally found to exist in the form of voids of different sizes in the spallation planes (Qi et al., 2011; Belak, 2004; Pei, 2013). In the spallation process, the dynamic behaviors, such as the nucleation rate of void, void growth velocity, coalescence of

voids, damage evolution rate and so on, are paramount importance and have been investigated persistently in experiments and theoretically in the last four decades (Qi et al., 2011; Belak, 2004; Pei, 2013; Seaman et al., 1976; Gurson, 1977; Johnson and Addessio, 1988; Curran et al., 1987; Strachan et al., 2001; Reina et al., 2011). However, up to date, owing to the lacking of effective in situ dynamic characterizations, it is still difficult to investigate the dynamic behaviors in the spallation process in experiments. Also, due to the obstacle brought by the cross-scale dynamic features of the spallation phenomena in the space and time, it is challenging to describe the spallation phenomena in theory. Because of the difficulties and challenges in both the experiments and theory, the spallation phenomena have not been understood well and the effective theoretical description is still an open problem.

\* Address: Center for High Pressure Science & Technology Advanced Research, 1690 Cailun Rd, Bldg #6, Pudong, Shanghai, 201203, PR China.

In this paper, the spallation process for the ductile metal under the plane shock loading is systematically discussed in theory. By means of the phase transition theory, non-equilibrium transport theory and the subsequent theoretical analysis, the conclusions are obtained: the spalling temperature, a new concept, is proposed first and the spallation critical behavior is proved to exist; the quantitative grain size, tensile strain rate and temperature dependence of both the damage evolution rate and the void growth velocity is obtained, i.e., a larger grain size, tensile strain rate and higher temperature will cause a larger damage evolution rate and void growth velocity; the existence of a characteristic size for the voids and a characteristic stress at the void boundary is discovered first, and their magnitude depend on the vacancy excitation energy and the average volume of one vacancy; the temperature for the metal adjacent to the growing void is found to be so high that it is possible to melt the metal, but it decreases quickly with the distance away from the void; the area of the plastic zone surrounding one formed spherical void is clarified; against the widely accepted viewpoint that the void growth is induced by the emission of dislocations (Belak, 2004), the distinctive viewpoint is put forward that when the shocking temperature approaches spalling temperature the void growth may arise from the agglomeration of vacancies rather than the emission of dislocations.

## 2. Theory and discussion

As is known, the spallation process is indeed one multi-scale problem. It composes of several main stages, void nucleation, void growth and void coalescence. For the different stages, the space scale crosses the microscale, meso-scale and macroscale and the time crosses many scales too. How can one theory describe the characters in the quite different scales? For the classical approach, it could describe some features in mesoscale or microscale. However, it fails to grasp the micro-properties of materials in the spallation process, because it is usually based on the continuum media assumption and often use the macro-variables instead of micro-variables. If one wants to capture the micro-characters, the quantum theory should be used. On the other hand, the phase transition theory and non-equilibrium theory in quantum mechanics could cover the multi-scale phenomena to some extent. So, to capture the micro-characters and describe the multi-scale spallation process, the quantum theories, phase transition theory and non-equilibrium theory are utilized.

Before the presentation of quantitative theory, the roles of vacancies in the spallation process should be discussed qualitatively first. For the shock-loaded ductile metal, the temperature and stress are incremented greatly. Consequently, a large number of vacancies may be yielded by the excitation of Frenkel defects, one vacancy and one concomitant interstitial atom, as shown in Fig. 1(a). Due to magnitude of the excitation energy  $\sim eV$ , the vacancies may enter the equilibrium state within the femto-second time and obey the distribution function  $\exp[-\varepsilon_n(\epsilon)/(2k_B T)]$  (Wang, 1993; Vainshtein et al., 2011),

where  $\varepsilon_n(\epsilon)$  is the strain  $\epsilon$  dependence of excitation energy,  $k_B$  is the Boltzmann constant,  $T$  is the temperature for the metal under the shock loading, and the factor 2 comes from the Boltzmann entropy increment. Initially, the yielded vacancies may be randomly distributed in the metal, as shown in Fig. 1(a). Afterwards, two series of rarefaction waves (left-propagated rarefaction waves and right-propagated rarefaction waves) generate and penetrate into the metals shown in Fig. 1(b). In the induced rarefaction zones, the remarkable stress and strain gradient appear. And the interstitial atoms tend to move to low-stress regions while the vacancies move to the high-stress regions (Vainshtein et al., 2011), such as the grain boundaries, then preferentially reside there. The diffusion velocity of the vacancies depend on the temperature and may reach observable value under the partial stress at relatively high temperatures in the rarefaction wave fronts. It should be emphasized that these processes have happened before the rarefaction wave fronts arriving at the planes where spallation will occur later. In this situation, the metal in these planes are still subjected to compression. As the rarefaction waves penetrate into the metals further and arrive at the planes, the metals will be released and tend to undergo the traction. As a result, the vacancies, initially distributed randomly, will be pushed to a narrow region termed spallation planes by the two series of rarefaction waves shown in Fig. 1(c). Hence, the high concentration of vacancies is formed in the spallation planes. And the vacancies may coalesce to form voids of different sizes (see Fig. 1(d)), thereby leading to the spallation in the planes.

For the metal after the shock loading, a high density of dislocations also emerges. The existence and motion of dislocations would alter the stress waves and the strain rate, then will affect the motion of vacancies further. In this theoretical description, the dislocation effect may be included by the altered stress and strain state.

### 2.1. Vacancy–vacancy interaction

Here the phase transition theory for ferromagnetic transition in condensed matter physics is utilized to describe the spallation process quantitatively. For this theory, the key is the effective interaction between any two vacancies and needs to be constructed first.

For the ductile metal, one existing vacancy will alter the electronic potential for the nearby itinerant electrons, resulting in the interaction  $\hat{V}_{ev}$  between electrons and vacancies, as shown in Fig. 2(a). Let field variables  $\Phi(\mathbf{R}), \Psi(\mathbf{r})$  denote the vacancy field and electron field, respectively.  $\rho(\mathbf{R}) = \Phi^*(\mathbf{R})\Phi(\mathbf{R}) = \sum_i \delta(\mathbf{R} - \mathbf{R}_i)$  gives the vacancy density. So, the electron–vacancy (e–v) interaction is (Gerald, 2000),

$$V_{ev} = \int d\mathbf{r} d\mathbf{R} \Phi^*(\mathbf{R})\Phi(\mathbf{R}) \hat{V}_{ev}(\mathbf{r} - \mathbf{R}) \Psi^\dagger(\mathbf{r})\Psi(\mathbf{r})$$

By means of the normal quantization steps, the e–v interaction could be written as,

$$V_{ev}(\mathbf{q}) = \sum_{i,\sigma,\mathbf{k},\mathbf{q}} e^{i\mathbf{q}\cdot\mathbf{R}_i} \hat{V}_{ev}(\mathbf{q}) C_{\mathbf{k}+\mathbf{q},\sigma}^\dagger C_{\mathbf{k},\sigma}$$

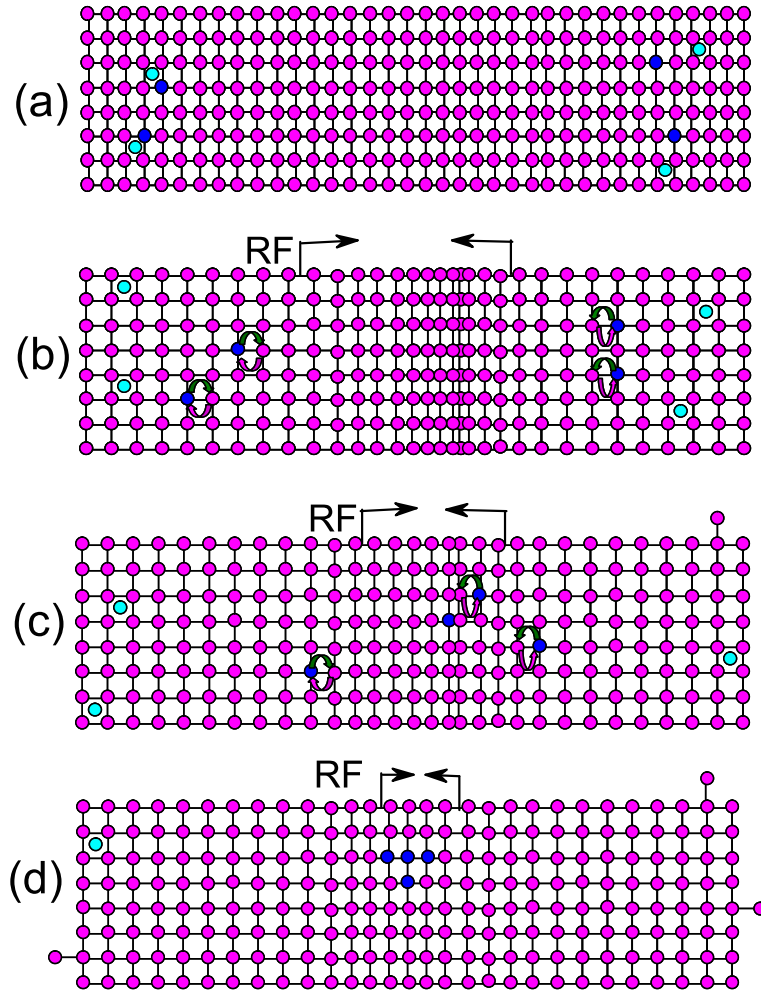


**Fig. 1.** Schematic diagrams of the dynamic processes before the two series of rarefaction waves arriving at the spallation planes: (a) the configurations of the atoms (pink circled), vacancies (blue circled) and interstitial atoms (light blue circled) in the metal after the shock loading; (b) the propagation of two series of rarefaction wave fronts (RF) and the motion of vacancies and atoms; the black arrows indicate the propagation of RF; (c) the formation of small void caused by the agglomeration of vacancies in the spallation planes; (d) the further growth of void due to the coalescence of vacancies. (For interpretation of the references to colour in this figure legend, the reader is referred to the web version of this article.)

where  $C_{\mathbf{k},\sigma}^\dagger, C_{\mathbf{k},\sigma}$  are the creation and destruction operators for the electron with momentum  $\mathbf{k}$  and spin  $\sigma$ , respectively. After eliminating the electron operators (see Fig. 2(b)), the effective vacancy–vacancy (v–v) interaction  $\hat{V}_{vv}(\mathbf{q})$  in the momentum space could be built:

$$\hat{V}_{vv}(\mathbf{q}) = \sum_{\mathbf{k}} \frac{2\hat{V}_{ev}^2(\mathbf{q})}{\varepsilon_{\mathbf{k}+\mathbf{q}} - \varepsilon_{\mathbf{k}}} f(\varepsilon_{\mathbf{k}+\mathbf{q}})[1 - f(\varepsilon_{\mathbf{k}})]$$

where  $f(\varepsilon_{\mathbf{k}})$  is the Fermi–Dirac (F–D) distribution function, and  $\varepsilon_{\mathbf{k}}$  is the kinetic energy of electrons. In the temperature range  $k_B T \ll \varepsilon_F$ , the v–v interaction could be approximated as,

$$\hat{V}_{vv}(\mathbf{q}) \approx -\frac{\hat{V}_{ev}^2(\mathbf{q})}{4\pi^2} \left(\frac{\hbar^2}{2m_e}\right)^{-3/2} \varepsilon_F^{1/2} \quad (1)$$

where  $\varepsilon_F$  is the Fermi energy and  $k_F$  the Fermi vector. Seen from Eq. (1), in the temperatures range  $k_B T \ll \varepsilon_F$ , the v–v

interaction exhibits the mutual attractive features. The attractive v–v interaction is rational, because as suggested by the calculated result (Gavini, 2008), the aggregation of two vacancies would decrease the total energy and form a more stable state.

## 2.2. Analogy-second order phase transition

To utilize the quantum statistical theory and simplify the theoretical treatment, the assumption that the vacancies stay in the equilibrium state is taken. And the non-equilibrium dynamic behaviors of spallation process is deferred later.

Combining with the obtained v–v interaction, in the Bloch representation, the whole Hamiltonian for the vacancies reads,

$$H = \sum_{\mathbf{k}} \frac{1}{2} (\varepsilon_{\mathbf{k}}(\varepsilon) + \varepsilon_n(\varepsilon)) b_{\mathbf{k}}^\dagger b_{\mathbf{k}} + \sum_{\mathbf{q}, \mathbf{k}, \mathbf{k}'} \hat{V}_{vv}(\mathbf{q}) b_{\mathbf{k}+\mathbf{q}}^\dagger b_{\mathbf{k}'-\mathbf{q}}^\dagger b_{\mathbf{k}'} b_{\mathbf{k}} \quad (2)$$

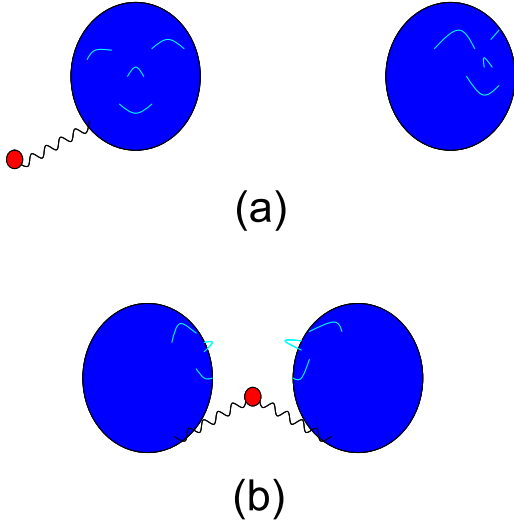


**Fig. 2.** Schematic diagrams of the interaction among voids (blue person): (a) non-interaction between the two voids; (b) the attraction induced by the electron (red circle) between the two voids. (For interpretation of the references to colour in this figure legend, the reader is referred to the web version of this article.)

where  $\varepsilon_{\mathbf{k}} = (\hbar\mathbf{k})^2/(2M_v)$  is the kinetic energy of vacancies,  $M_v$  is the effective mass of the vacancy, about  $10^2$  times of the electron mass  $m_e$  because of  $\varepsilon_{\Lambda} \approx 0.01$  eV ( $\Lambda = \pi/a$  is the reciprocal wave vector, and  $a$  is the lattice parameter), the typical vibration energy for atoms, i.e., phonon energy.  $\varepsilon_n(\epsilon)$  is the strain  $\epsilon$  dependence of excitation energy ( $\sim$  eV) for the vacancy. In addition, for the kinetic energy of vacancies,  $\varepsilon_{\mathbf{k}}(\epsilon) = \varepsilon_{\mathbf{k}+\Lambda}(\epsilon)$  holds due to the transfer symmetry in the crystal. The prepositive factor 1/2 in the first term in Eq. 2 originates from the denominator 2 in the distribution function  $\exp[-(\varepsilon_{\mathbf{k}}(\epsilon) + \varepsilon_n(\epsilon))/2k_B T]$ .  $b_{\mathbf{k}}^{\dagger}, b_{\mathbf{k}}$  signify the creation and destruction operators for the vacancy with wave vector  $\mathbf{k}$ . They are the boson operators and obey the Bose–Einstein (B–E) distribution. Here it is reasonable, because the B–E distribution are close to the Boltzmann distribution in the temperature range  $k_B T \ll \varepsilon_n(\epsilon)$ .

In the coherent state representation (John and Henri, 1998), the partition function for the vacancies in the equilibrium state is,

$$Z = \int D(\phi^*(\mathbf{k})\phi(\mathbf{k})) e^{-\int \phi^*(\mathbf{k}) \frac{1}{2} (\bar{\varepsilon}_{\mathbf{k}}(\epsilon) + \bar{\varepsilon}_n(\epsilon)) \phi(\mathbf{k}) \frac{d\mathbf{k}}{(2\pi)^3} - \int \phi^*(\mathbf{k}+\mathbf{q}) \phi^*(\mathbf{k}'-\mathbf{q}) \bar{V}_{vv}(\mathbf{q}) \phi(\mathbf{k}') \phi(\mathbf{k}) \frac{d\mathbf{k} d\mathbf{q}}{(2\pi)^9}}$$

where  $\beta = 1/(k_B T)$ ,  $\bar{\varepsilon}_{\mathbf{k}}(\epsilon) = \beta \varepsilon_{\mathbf{k}}(\epsilon)$ ,  $\bar{\varepsilon}_n(\epsilon) = \beta \varepsilon_n(\epsilon)$ ,  $\bar{V}_{vv}(\mathbf{q}) = \beta \hat{V}_{vv}(\mathbf{q})$ .

The effective interaction  $\bar{V}_{vv}(\mathbf{q})$  may be expanded as  $\bar{V}_{vv}(\mathbf{q}) = \bar{V}_{vv}(0) + \bar{V}'_{vv}(0)\mathbf{q} + \frac{1}{2}\bar{V}''_{vv}(0)\mathbf{q}^2 + \dots$ . For simplicity, the first term in the expansion, independent of wave vector, is taken into account only. Using the random phase approximation, the self-energy  $\Sigma(\mathbf{k})$  of vacancy is,

$$\Sigma(\mathbf{k}) \approx -\frac{\bar{V}_{vv}(0)}{3\pi^2} \frac{\Lambda^3}{\bar{\varepsilon}_n(\epsilon)}$$

For the vacancy, the re-normalized zero excitation energy  $\varepsilon_n(\epsilon)$ , indicating the infinite correlation length among them, suggests the happening of second-order phase transition (John and Henri, 1998; Yang, 2007). Therefore, the phase-transition critical behaviors emerge.

$$\frac{1}{2} \bar{\varepsilon}_n(\epsilon) - \Sigma(\mathbf{k}) = 0$$

The transition temperature could be obtained,

$$k_B T_t = -\frac{3\pi^2}{2\Lambda^3 \hat{V}_{vv}(0)} \varepsilon_n^2(\epsilon) \quad (3)$$

Substitute Eq. (1) into Eq. (3),

$$k_B T_t = \frac{6\pi^4 \varepsilon_n^2(\epsilon)}{\Lambda^3 V_{ev}^2(0)} \left( \frac{\hbar^2}{2m_e} \right)^{-3/2} \varepsilon_F^{-1/2}$$

If the screened coulomb interaction  $4\pi Ze^2/(q^2 + r_{es}^{-2})$  is taken as the e–v interaction  $V_{ev}(q)$ , where  $r_{es}^{-2}$  is the electronic screening length and  $Z$  the effective charge of one vacancy, here the transition temperature named spalling temperature is

$$k_B T_t = \frac{3}{8} \frac{4}{Z^2} \left( \frac{k_F}{\Lambda} \right)^3 \frac{\varepsilon_n^2(\epsilon)}{\varepsilon_F}$$

Which means that the complete spallation occurs when the shocked temperature is higher than the spalling temperature  $T_t$ .

This is the phase transition theory resorted to describe the spallation processes. It is like the ferromagnetic transition, composed of the processes, the nucleation, growth and percolation of magnetic domains. For the validity of this theory, the existence of spallation critical behaviors confirmed by the experiments (Qi et al., 2007; Qi et al., 2012) may verify the theory. Besides the critical behaviors, it may also predict that the spallation critical parameters are the same constants for the different types of ductile metals with different spalling temperatures, although the critical parameters are difficult to obtain. This prediction needs to be proved by the future experiments.

The following sections will focus on the dynamic properties in the spallation process further.

For the spallation process, the large stress and strain gradient appear in the spallation planes, when the catching

rarefaction waves and the reflected rarefaction waves interconnect. These would lead to the dynamic properties of spallation. To describe them, the semi-classical Boltzmann equation is employed here (Phillips, 2003),

$$\begin{aligned} \frac{\partial \mathbf{g}_{\mathbf{k}}}{\partial t} \Big|_{\text{coll}} = & \frac{\partial \mathbf{g}_{\mathbf{k}} - v_0(\epsilon)}{\hbar} \nabla_{\mathbf{r}} P(\mathbf{r}) \\ & + \frac{\mathbf{g}_{\mathbf{k}} \dot{\mathbf{r}}}{2k_B T} \left[ (\varepsilon_{\mathbf{k}}(\epsilon) + \varepsilon_n(\epsilon)) \frac{\nabla_{\mathbf{r}} T(\mathbf{r}(t))}{T} - \frac{\partial \varepsilon_n(\epsilon)}{\partial \epsilon} \nabla_{\mathbf{r}} \epsilon(\mathbf{r}(t)) \right] \end{aligned} \quad (4)$$

where  $g_{\mathbf{k}}$  is the abbreviation of the temperature  $T(\mathbf{r})$ , strain  $\epsilon(\mathbf{r})$  and momentum  $\mathbf{k}$  dependence of distribution function  $g(\mathbf{k}, T(\mathbf{r}), \epsilon(\mathbf{r})) = \exp[-(\epsilon_{\mathbf{k}}(\epsilon) + \epsilon_n(\epsilon))/2k_B T]$  for the vacancies. In Eq. (4), the first term on the right comes from the stress gradient field, accelerating the vacancies  $\hbar \mathbf{k} \approx -v_0(\epsilon) \nabla_{\mathbf{r}} P(\mathbf{r})$ , where  $v_0(\epsilon)$  is the vacancy volume and  $P(\mathbf{r})$  the stress field. The second and third term in the square brackets arise from the temperature and strain gradient fields, respectively. They all contribute to the diffusion of vacancies.

Using the relaxation time approximation,  $\partial g / \partial t|_{coll} = -(g_{\mathbf{k}} - g_{\mathbf{k}}^0) / \tau_{\mathbf{k}} = -g_{\mathbf{k}}^0 / \tau_{\mathbf{k}}$ , where  $g_{\mathbf{k}}^0$  is the equilibrium distribution function for the vacancies and  $\tau_{\mathbf{k}}$  is the corresponding relaxation time. Ignoring the phase coherence among the scattering of different mechanisms, the relaxation time  $\tau_{\mathbf{k}}$  could be approximated as  $1/\tau_{\mathbf{k}} = 1/\tau_{b\mathbf{k}} + 1/\tau_{v\mathbf{k}}$ , where  $1/\tau_{b\mathbf{k}}$  arises from the scattering between the vacancies and the grain boundaries, and  $1/\tau_{v\mathbf{k}}$  results from the scattering among the vacancies. In the polycrystalline metals with the grain sizes, typically  $L \sim 100$  microns, the scattering rate, originating from the vacancy-grain boundary scattering for the vacancies with the velocity  $\mathbf{v}_{\mathbf{k}}$ , is  $\mathbf{v}_{\mathbf{k}}/L$ . And the elastic free length, one vital parameter for the vacancies, is  $l_{\mathbf{k}} = \mathbf{v}_{\mathbf{k}} \tau_{v\mathbf{k}}$ .

According to the Fermi golden rule, the relaxation time  $\tau_{v\mathbf{k}}$  determined by the Umklapp scattering processes among vacancies is,

$$\frac{-g_{\mathbf{k}}^1}{\tau_{v\mathbf{k}}} = \frac{2\pi}{\hbar} \sum_{\mathbf{k}', \mathbf{q}} |\hat{V}_{v\mathbf{v}}(\mathbf{q})|^2 \left[ g_{\mathbf{k}} g_{\mathbf{k}'} (1 + g_{|\mathbf{k}+\mathbf{q}|-\Lambda}) (1 + g_{\mathbf{k}'-\mathbf{q}}) - g_{|\mathbf{k}+\mathbf{q}|-\Lambda} g_{\mathbf{k}'-\mathbf{q}} (1 + g_{\mathbf{k}}) (1 + g_{\mathbf{k}'}) \right] \times \Theta(|\mathbf{k} + \mathbf{q}| - \Lambda) \delta(\epsilon_{\mathbf{k}} + \epsilon_{\mathbf{k}'} - \epsilon_{|\mathbf{k}+\mathbf{q}|-\Lambda} - \epsilon_{\mathbf{k}'-\mathbf{q}})$$

where the function  $\Theta(x)$  satisfies  $\Theta(x) = \begin{cases} 1, & \text{for } x \geq 0 \\ 0, & \text{others} \end{cases}$ . Here the contributions to the vacancy scattering from other processes, such as the scattering between dislocations and vacancies, the new generation and re-combination of both the vacancies and interstitial atoms, are not considered. Then one may obtain the vacancy current density (VCD)  $j$ ,

$$j = \int \frac{\mathbf{v}_{\mathbf{k}} \tau_{\mathbf{k}} g_{\mathbf{k}}^0}{2k_B T} \left[ (\epsilon_{\mathbf{k}}(\epsilon) + \epsilon_n(\epsilon)) \frac{\mathbf{v}_{\mathbf{k}} \cdot \nabla_{\mathbf{r}} T(\mathbf{r}(t))}{T} - \frac{\partial \epsilon_n(\epsilon)}{\partial \epsilon} \mathbf{v}_{\mathbf{k}} \cdot \nabla_{\mathbf{r}} \epsilon(\mathbf{r}(t)) + v_0(\epsilon) \mathbf{v}_{\mathbf{k}} \cdot \nabla_{\mathbf{r}} P(\mathbf{r}) \right] \frac{d\mathbf{k}}{(2\pi)^3} \quad (5)$$

where  $B_0$  is the Young's modulus,  $\dot{\epsilon}$  is the tensile strain rate and  $\mathbf{v}_{\mathbf{k}} \cdot \nabla_{\mathbf{r}} P(\mathbf{r})$  may approximate  $B_0 \dot{\epsilon}$ . For the ductile metal after shock loading, a considerable density of dislocations is also yielded. The dislocations influence the stress, strain and strain rate during the spallation process. Further, the altered stress and strain field affect the motion of vacancies. This detailed dislocation effect on the motion of vacancies may be important and needs to be investigated further. But here the dislocation effects could be covered by the stress, strain and strain rate in the theories.

For the directional VCD, the stress gradient may be governing. And at the temperature zone  $\sim 10^3$  K, much lower than the characteristic excitation energy  $\epsilon_n(\epsilon)$ , the scatter-

ing among vacancies may be quite weak. So the elastic free length  $l_{\mathbf{k}}$  may be larger than the grain sizes  $L$ , making the relaxation time  $\tau_{\mathbf{k}}$  determined by the grain sizes.

$$j \approx \frac{L v_0(\epsilon) B_0 \dot{\epsilon}}{6k_B T} \frac{\Lambda^3}{6\pi^2} e^{-\frac{\epsilon_n(\epsilon)}{2k_B T}} \quad (6)$$

Seen from Eq. (6), the VCD is notably sensitive to the excitation energy  $\epsilon_n(\epsilon)$  and the temperature. And it also hinges on the tensile strain rate and the grain sizes, i.e., the larger the grain sizes, the larger the VCD and vice versa. The VCD, affected by these factors, may determine many dynamic properties of spallation, including the damage evolution rate, nucleation rate, void growth velocity and so on, which will be discussed in the following sections. If the typical parameters  $T \sim 10^3$  K,  $\epsilon_n(\epsilon) \sim 1$  eV and  $L \sim 10^{-4}$  m are taken, the VCD could reach  $10^{28}/\text{m}^2 \text{ s}$ .

### 2.3. Damage evolution rate

In the spallation planes, one may obtain the damage evolution rate  $\dot{V}$  in terms of the VCD,

$$\dot{V} = 2jSv_0(\epsilon) \quad (7)$$

where  $S$  is the cross section of spallation planes and the factor 2 originates from the two series of rarefaction waves. Actually, the tensile stress and strain rate monitored by the respective series of rarefaction waves are different. Here for simplicity, the difference is not discussed. Substitute equation (6) into Eq. (7), it is

$$\dot{V} = \frac{LSv_0^2(\epsilon) B_0 \dot{\epsilon}}{3k_B T} \frac{\Lambda^3}{6\pi^2} e^{-\frac{\epsilon_n(\epsilon)}{2k_B T}} \quad (8)$$

According to Eq. (8), the damage evolution rate rely on the tensile strain rate and the grain size. A larger tensile strain rate and grain size would lead to a higher damage evolution rate.

### 2.4. Stress at the void boundary

The large number of vacancies in the spallation planes would continuously coalesce to form the growing voids and release a large amount of energy at the void boundary. In this case, the expanding void boundary may not be free and the released energy may lead to the effective stress  $P_b$  at the expanding void boundary. If the void expands by  $dr$  in radius, the work  $P_b 4\pi r^2 dr$  done by the stress may be equal to the released energy  $1/2 \epsilon_n(\epsilon) 4\pi r^2 dr / v_0(\epsilon)$ . So, for the stably growing void, the stress at the void boundary  $P_b$  is

$$P_b = \frac{1}{2} \frac{\epsilon_n(\epsilon)}{v_0(\epsilon)} \quad (9)$$

Based on Eq. (9), the stress  $P_b$ , independent of void size and void growth velocity, is one intrinsic characteristic parameter, and it only depends on the type of metal. For the materials with the fracture toughness  $K_{IC}$  around the void, one may find the critical radius  $R_c$  for the stably growing voids,

$$R_c = \frac{1}{\pi} \left( \frac{K_{IC}}{P_b} \right)^2 \quad (10)$$

The critical radius  $R_c$  means that once the radius of void approaches  $R_c$ , the cracks may be generated at the void boundary. So the radius of spherical void can not exceed  $R_c$ .

Here the existence of effective pressure needs to be proved by experiments in the future. For instance, if the lattice strain near the void could be observed clearly in the dynamic spallation process, it will be very helpful for clarifying this point.

### 2.5. Plastic zone around the void

For the monatomic ductile metal, the stress  $P_b$  generally exceeds the yield strength of metal and therefore generates a plastic zone surrounding the voids as shown in Fig. 3. Through the simple calculation (Reina et al., 2011), one may obtain the stress fields around the growing void.

$$P_r(r) = A + \frac{B}{r^3} \text{ and } P_\theta(r) = A - \frac{B}{2r^3}$$

where  $P_r(r)$ ,  $P_\theta(r)$  are the radial stress and tangential stress, respectively.  $A$  and  $B$  are the parameters to be determined. By using the boundary conditions,  $P_r(r_0) = P_b$ ,  $P_r(R_0) - P_\theta(R_0) = Y$ , where  $Y$ ,  $r_0$  are the yield strength and the radius of void, and the fact  $P_b \gg Y$ , the outer radius  $R_0$  of the plastic zone could be obtained,

$$R_0 = \sqrt[3]{\frac{3P_b}{2Y}}r_0 \quad (11)$$

Here the calculation for the void is reasonable, because the expanding velocity of void is much smaller than the sound velocity.

Substituting Eq. (9) into Eq. (11) yields

$$R_0 = \sqrt[3]{\frac{3\epsilon_n(\epsilon)}{4Yv_0}}r_0$$

### 2.6. Nucleation and growth of void

By clarifying the stress and plastic zone surrounding the void, let us turn to the nucleation rate and the void growth

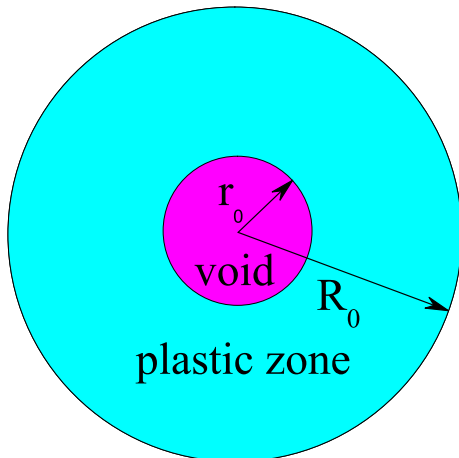


**Fig. 3.** Schematic diagram of the void (pink circled) with the radius  $r_0$  and the surrounding plastic zone (light blue) with the radius  $R_0$ . (For interpretation of the references to colour in this figure legend, the reader is referred to the web version of this article.)

velocity. The nucleation and the growth of voids are the sources of dynamic damage in the spallation planes. So

$$\dot{V} = \sum_i \left[ \frac{dn_i}{dt} \frac{4\pi}{3} r_i^3 + n_i 4\pi r_i^2 \frac{dr_i}{dt} \right] \quad (12)$$

where  $n_i$  is the number of voids with radius  $r_i$ . At the beginning of spallation process, the nucleation maybe the dominant factor. And inserting Eq. (8) into Eq. (12) would lead to the nucleation rate for the nanometer sized void:

$$\frac{dn_i}{dt} = \frac{LSv_0^2(\epsilon)B_0\dot{\epsilon}}{12k_B T r_i^3} \frac{\Lambda^3}{2\pi} e^{-\frac{\epsilon_n(\epsilon)}{2k_B T}} \quad (13)$$

Here the calculation only considers the contribution to the nucleation by the diffusion and agglomeration of vacancies and disregards other factors, e.g., the boundaries, the second-phase particles, the impurities and so on. Whether it captures the main point of nucleation or not still needs to be proved by experiments further despite of the difficulty in experiments.

In the following processes, the void growth may dominate the damage evolution and thus the newly void nucleation is subsidiary. Considering that the vacancies diffusing into the plastic zone will enter the void in terms of plastic fluid or radial acceleration, the growth velocity for the void with radius  $r_0$  could be obtained,

$$\dot{r}_0 \approx \frac{1}{2} j v_0(\epsilon) \sqrt[3]{\left(\frac{3P_b}{2Y}\right)^2} \quad (14)$$

Eqs. (6), (9) and (14) yield

$$\dot{r}_0 \approx \frac{Lv_0(\epsilon)B_0\dot{\epsilon}}{12k_B T} \frac{\Lambda^3}{6\pi^2} \sqrt[3]{\frac{9\epsilon_n^2(\epsilon)v_0(\epsilon)}{16Y^2}} e^{-\frac{\epsilon_n(\epsilon)}{2k_B T}} \quad (15)$$

which shows that the void growth velocity is proportional to the tensile strain rate and the grain size. According to the expression of the VCD and void growth velocity, they strongly rely on the tensile strain rate and the temperature of metal after shock loading. If the tensile strain rate reaches  $10^6/s$ , the VCD may achieve  $\sim 10^{29}/(m^2 s)$  and may result in the void growth velocity  $\sim 100 m/s$ . Actually, the growing void may link up the initial small voids in its plastic zone and form a larger void. If this is taken into account, the corrected void growth velocity  $\dot{r}_c$  is

$$\dot{r}_c \left( 1 - \int_0^t \frac{\dot{V}}{V_0} dt \right) \approx \frac{Lv_0(\epsilon)B_0\dot{\epsilon}}{12k_B T} \frac{\Lambda^3}{6\pi^2} \sqrt[3]{\frac{9\epsilon_n^2(\epsilon)v_0(\epsilon)}{16Y^2}} e^{-\frac{\epsilon_n(\epsilon)}{2k_B T}}$$

where  $V_0$  is the initial undamaged volume in the spallation planes. In actuality, the damage evolution exhibits the time dependence. But for simplicity, it is assumed to be constant and the corrected void growth velocity  $\dot{r}_c$  is,

$$\dot{r}_c = \frac{Lv_0(\epsilon)B_0\dot{\epsilon}}{12\left(1 - \frac{\delta t}{t_f}\right)k_B T} \frac{\Lambda^3}{6\pi^2} \sqrt[3]{\frac{9\epsilon_n^2(\epsilon)v_0(\epsilon)}{16Y^2}} e^{-\frac{\epsilon_n(\epsilon)}{2k_B T}} \quad (16)$$

where  $\delta$  is the final damage fraction in the spallation planes, equal to  $\dot{V}t_f/V_0$ , and  $t_f$  is the duration time of the whole spallation process. For the complete spallation, the damage fraction is  $\delta = 1$ .

To estimate the void growth velocity for the tantalum and compare with the simulation result  $\sim 200$  m/s estimated for the largest void (Strachan et al., 2001), the parameters (De Boer et al., 1988),  $\varepsilon_n(\epsilon) \sim 2.9$  eV,  $L \sim 16 \times 53.3$  Å,  $T \sim 3 \times 10^3$  K,  $\dot{\epsilon} \sim 2.7 \times 10^{10}$  /s estimated from the simulation for the largest void (Strachan et al., 2001), the volume of one vacancy  $v_0(\epsilon) \approx 18 \times 10^{-30}$  m<sup>3</sup>, the yield strength  $Y = 0.77$  GPa, are taken. The estimated void growth velocity is  $\dot{r}_c \sim 130$  m/s, which agrees with the simulation result  $\sim 200$  m/s.

## 2.7. Estimation of temperature

For the metals around the void, three main dissipation mechanisms exist for the work done by the expanding void boundary. One is the elastic deformation energy, the second one is the kinetic energy of atoms and the last one is the plastic heat. And other types of dissipation energy may be much more tiny. The elastic deformation energy and the kinetic energy may occupy only several percent of the total work according to a simple estimation. So the work may mainly dissipate into the plastic heat. Therefore, for the estimation of the temperature field distribution around the void, the energy-conservation law is used:

$$V(r)C_v dT(r, t) = dU(r) = dQ(r) - P(r)dV(r)$$

where  $V(r)$  is the volume at the distance  $r$  from the center of void,  $C_v$  is the specific heat capacity,  $dU(r)$  is the variation of internal energy,  $dQ(r)$  is the transport thermal energy and  $-P(r)dV(r)$  is the work done. In terms of the simple derivation, the time and distance dependence of temperature field  $T(r, t)$  around the void obey

$$2 \frac{P_b r_0^3}{r^4} \frac{dr}{dt} = C_v \frac{\partial T(r, t)}{\partial t} - K \frac{\partial^2 T(r, t)}{\partial r^2} - \frac{2}{r} K \frac{\partial T(r, t)}{\partial r} \quad (17)$$

where the radial velocity is (Wang, 2005)  $dr/dt = \dot{r}_0 r_0^2 / r^2$ , and  $K$  is the thermal conductivity. Here only the rough estimation is done. Due to the much larger thermal transport velocity than the expanding velocity of void  $\dot{r}_0$ , the temperature field is approximated to be no time dependence. So the distance dependence of temperature field is

$$T(r) \approx T(R_0) + \frac{P_b r_0^3 \dot{r}_0}{4K} \left( \frac{1}{r^4} - \frac{1}{R_0^4} \right)$$

As shown in this equation, the temperature decreases quickly with the distance from the center of void. By inserting the parameters for aluminium (Martienssen and Warlimont, 2005)  $K \approx 240$  W/(m K),  $r_0 \sim 40$  μm, the strain rate  $\sim 10^5$  /s,  $\dot{r}_0 \sim 10$  m/s into this equation, the obtained temperature at the void boundary is  $T(r_0) \approx T(R_0) + 1200$  K. The temperature is so high that it is possible to melt the aluminium.

In the above theoretical treatment and discussions, the factors, particularly the crystalline orientations of single crystal and grain boundaries in the polycrystal which may affect the strain rates and the effective mass of vacancies, are not considered. In reality, the grain boundaries may be easy to situate the vacancies and voids, and therefore the cracks form along the grain boundaries, causing the spallation further. This paper mainly focuses on

vacancy effects on the spallation of metal under shock loading, which is at high strain rates and relatively high temperatures, not referring to the case of low strain rates and low temperatures. Also, the structural phase transition under loading has not been considered in this work. These effects on spallation need to be investigated further.

The theories in the paper may only apply for the case of high shocking temperature and high strain rates. When the shocking strain rates and shocking temperature is low, the vacancy concentration is low and the corresponding diffusion velocity is expected to be small. In this case, the dislocations may dominate the spallation processes while the vacancy effects may be subsidiary. However, when the shocking temperature and strain rates is high, the concentration and diffusion velocity of vacancies may be high. In this case, the vacancies may dominate the spallation processes. Combined with the different roles of vacancies in the two cases of low temperature, low strain rate, and high strain rate, high temperature, expectedly, the crossover for the spallation mechanism may exist near the cutoff temperature or strain rate. Considering the importance of shocking temperature for the concentration and diffusion velocity of vacancies, the shocking temperature rather than the strain rate may be more suitable for characterizing the crossover. That is, when the shocking temperature approaches the spalling temperature, the crossover of spallation mechanism may occur and the coalescence and diffusion of vacancies may monitor the spallation process.

## 3. Conclusions

In summarized, the spallation process for the ductile metals under plane shock loading is discussed in theory. By employing the phase transition theory and non-equilibrium transport theory, the spallation process may be understood as a result of the diffusion and agglomeration of the generated vacancies. Through the detailed theoretical analysis, the following important points are concluded for the dynamic spallation process: (1) the spalling temperature, a new concept, is proposed first and the appearance of spallation critical behavior is proved; (2) the quantitative grain size, tensile strain rate and temperature dependence of both the damage evolution rate and the void growth velocity is obtained; (3) the existence of a characteristic size for the voids and a characteristic stress at the void boundary is discovered first, and their magnitude depend on the vacancy excitation energy and the average volume of one vacancy; (4) the temperature of metal near the growing void is found to be high, possibly causing the metal to melt, and it decreases quickly with the distance away from the void; (5) the area of the plastic zone surrounding one formed spherical void is clarified; (6) the viewpoint is put forward that the void growth may arise from the agglomeration of vacancies rather than the emission of dislocations at relatively high temperatures and strain rates. Most of the above theoretical results are novel and obtained first.

## Acknowledgements

The author is grateful to colleagues Guangfu Ji, Hongliang He, Wenjun Zhu and Liang Wang for the helpful discussions and the amounts of provided information.

## References

- Pei, X.Y., 2013. Study on damage evolution dynamics for the dynamic tensile failure (Spallation) of high-pure OFHC[D], p. 38.
- Qi, M.L., Zhong, S., Fan, D., Luo, C., He, H.L., 2011. *Chin. Phys. Lett.* 28, 016103.
- Belak, J., et al., 2004. Incipient spallation fracture in light metals from 3D X-Ray tomography, 2D microscopy, and molecular dynamics simulations. UCRL-CONF-204946.
- Gurson, A.L., 1977. *Trans. ASME J. Eng. Mater. Technol.* 99, 2–15.
- Seaman, L., Curran, D.R., Shockey, D.A., 1976. *J. Appl. Phys.* 47, 4814.
- Johnson, J.N., Addessio, F.L., 1988. *J. Appl. Phys.* 64 (12), 6699.
- Curran, D.R., Seaman, L., Shockey, D.A., 1987. *Phys. Rep.* 147 (5–6), 253.
- Strachan, A., Cagin, T., Goddard, W.A., 2001. *Phys. Rev. B* 63, 060103R.
- Reina, C., Marian, J., Ortiz, M., 2011. *Phys. Rev. B* 84, 104117.
- Wang, Zhicheng, 1993. *Thermodynamics, Statistical Physics*, second ed. Higher education press, Beijing, p. 271.
- Vainshtein, Boris K., Fridkin, Valdimir M., Indenbom, Valdimir L., 2011. *Modern Crystallography 2, Structure of Crystals* (Ziqin Wu and Chen Gao translate, University of Science and Technology of China Press, 2011), pp. 304–307.
- Mahan, Gerald D., 2000. *Many-Particle Physics*, third ed. Kluwer Academic/Plenum Publishers, pp. 14–23.
- Gavini, V., 2008. *Phys. Rev. Lett.* 101, 205503.
- Negele, John W., Orland, Henri, 1998. *Quantum Many-Particle Systems*. Westview press, pp. 20–200.
- Zhanru, Yang, 2007. *Quantum Statistical Physics*. Higher Education Press, p. 313.
- Qi, M.L., Qin, X.Y., Zhang, L., He, H.L., Yan, S.L., 2007. *J. Wuhan Univ. Technol.* (2).
- Qi, M.L., Luo, C., He, H.L., et al., 2012. *J. Appl. Phys.* 111 (4), 043506.
- Phillips, Philip, 2003. *Advanced Solid State Physics*. Westview Press, p. 188.
- De Boer, F.R., Boom, R., Mattens, W.C.M., Miedema, A.R., Niessen, A.K., 1988. *Cohesion in Metals*. North-Holland, Am-sterdam.
- Wang, L.L., 2005. *Foundation of Stress Waves*, second ed. National Defense Industry Press, p. 239, [in Chinese].
- Martienssen, W., Warlimont, H. (Eds.), 2005. *Springer Handbook of Condensed Matter and Materials Data (I)*. Springer, Berlin Heidelberg, p. 81.